iScience

CellPress
OPEN ACCESS

Article

Network pharmacology and experimental validation to reveal the target of matrine against PRRSV

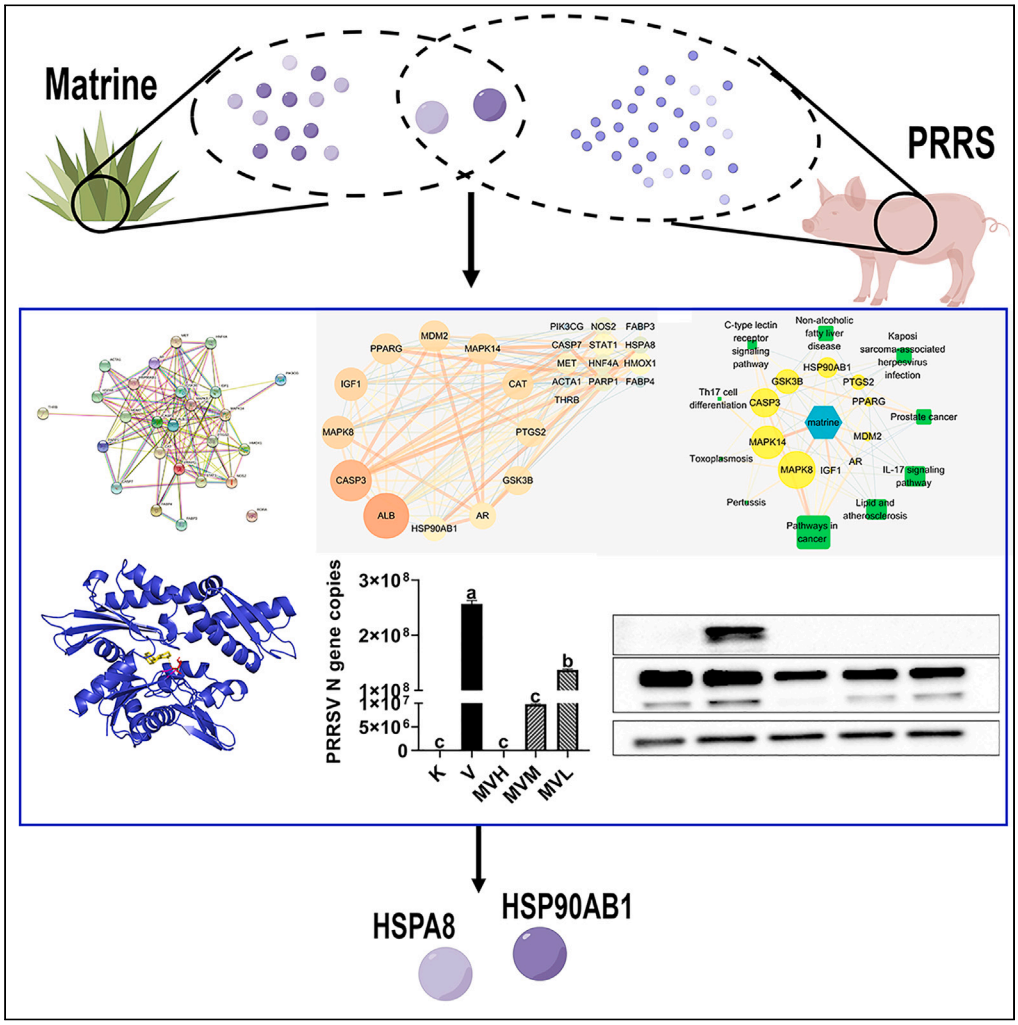

Yaxiang Zhao, Xiaoya Ling, Hua Zhang, ..., Jianzhong Wang, Hongquan Li, Na Sun

snzh060511@126.com

Highlights

Network pharmacology and molecular docking were used to identify targets of matrine

The down-regulation effect of matrine on HSPs was revealed by *in vitro* experiments

The up-regulation of HSPs expression was caused by PRRSV infection

Zhao et al., iScience *26*, 106371
April 21, 2023
https://doi.org/10.1016/j.isci.2023.106371

iScience

CellPress
OPEN ACCESS

Article

Network pharmacology and experimental validation to reveal the target of matrine against PRRSV

Yaxiang Zhao,[1] Xiaoya Ling,[1] Hua Zhang,[1] Panpan Sun,[1] Yaogui Sun,[1] Wei Yin,[1] Kuohai Fan,[2] Huizhen Yang,[1] Jia Zhong,[1] Zhenbiao Zhang,[1] Jianzhong Wang,[1] Hongquan Li,[1] and Na Sun[1,3,*]

SUMMARY

Porcine reproductive and respiratory syndrome (PRRS) is an epidemic animal infectious disease worldwide. In our previous research it was suggested that matrine could inhibit PRRSV infection both *in vitro* and *in vivo*, but the antiviral mechanisms are still undecided. Network pharmacology can well solve the difficult problem of "multiple targets, multiple pathways" in the research of TCM action targets. The results of network pharmacology indicated that matrine exerts its anti-PRRSV effect by targeting HSPA8 and HSP90AB1. The results of real-time fluorescent quantitative PCR and western blot showed that infection with PRRSV induced a significant increase in the expression of HSPA8 and HSP90AB1 whereas matrine treatment could significantly reverse it, and the number of viruses of PRRSV also decreased. In this study, the method of network pharmacology was used to explore HSPA8 and HSP90AB1 which were the potential targets of matrine against PRRSV on Marc-145 cells.

INTRODUCTION

The "mystery swine disease" was first discovered in the United States and was later well-defined as porcine reproductive and respiratory syndrome (PRRS). In addition, its causative agent was a porcine reproductive and respiratory syndrome virus (PRRSV).[1,2] In 1996, the first discovery of PRRSV and the existence of PRRS was confirmed in China. From the years 2006–2016, the prevalent strain of PRRSV in China gradually progressed from HP-PRRSV to NADC34-like PRRSV.[3,4] Researcher Fang founded in an epidemiological survey from the years 2017–2021 that the prevalent strain in southern China was still HP-PRRSV and the phenomenon of mixed infection of different types of straining widely exists in large-scale farms.[5] The significant method to control PRRS is to immunize pigs with vaccines. However, because of the immunosuppressive characteristics of PRRSV, the effect of vaccine immunization is limited.[6] Therefore, the progress of a new type of anti-PRRSV drug has become the focus of researchers.

Natural compounds derived from traditional Chinese medicine that has antiviral effects and have become the hotspot.[7,8] Matrine is an alkaloid extracted from the rhizomes of Sophora Radix and Rhizoma Sophorae. Our previous research has confirmed that matrine possessed anti-PRRSV activities both *in vitro* and *in vivo* and its antiviral mechanisms involve inhibiting PRRSV replications, directly inactivating PRRSV, and interfering with PRRSV-induced apoptosis.[9] However, because of the lesser known specific targets, the antiviral mechanisms of matrine's anti-PRRSV action have not yet been explained clearly.

In this study, network pharmacology combined with molecular docking was used to screen potential targets of matrine for its anti-PRRSV effect and matrine was used to treat PRRSV-infected Marc-145 cells to validate the predicted results.

RESULTS

Anti-PRRSV targets of matrine

259 potential targets of matrine were collected through the PharmMapper database (Table S1). 824 PRRS-related disease targets were collected through the Comparative Toxicogenomics Database (CTD) (Table S2). Finally, by taking the intersection of the above drug targets and disease targets,

[1]Shanxi Key Laboratory for Modernization of TCVM, College of Veterinary Medicine, Shanxi Agricultural University, Taigu, Shanxi 030801, China

[2]Laboratory Animal Center, Shanxi Agricultural University, Taigu, Shanxi 030801, China

[3]Lead contact

*Correspondence: snzh060511@126.com

https://doi.org/10.1016/j.isci.2023.106371

Table 1. The potential targets of matrine anti-PRRSV

Number	Gene symbol	Number	Gene symbol	Number	Gene symbol
1	ACTA1	10	HMOX1	19	NOS2
2	ALB	11	HNF4A	20	PARP1
3	AR	12	HSP90AB1	21	PIK3CG
4	CASP3	13	HSPA8	22	PPARG
5	CASP7	14	IGF1	23	PTGS2
6	CAT	15	MAPK14	24	RORA
7	FABP3	16	MAPK8	25	STAT1
8	FABP4	17	MDM2	26	THRB
9	GSK3B	18	MET		

a total of 26 potential targets related to the anti-PRRSV effect of matrine were obtained (Table 1, Figure 1).

PPI network of targets

Twenty-six potential targets were input into the String database, the "Organisms" was set as "Homo sapiens", and then the protein interaction network was productivity (Figure 2A). Cytoscape 3.7.2 software was used to construct a PPI network. After topological analysis of the network, the core target screening criteria were set as Degree Un-Dir >11.04. A total of 12 core targets were obtained, such as (Figure 2B) within the range of the red box: ALB, CASP3, MAPK8, IGF1, CAT, MAPK14, MDM2, PPARG, GSK3B, PTGS2, AR, and HSP90AB1.

GO and KEGG pathway analysis

Twenty-six potential targets were entered in the DAVID database, and a total of 202 GO enrichment results were obtained (Table S3). The enrichment results were sorted according to the p-value, and the top 10 results were selected for plotting (Figure 3A). Biological processes mainly involved for "response to the drug" and "response to xenobiotic stimulus". For cell components, proteins associated with "nucleoplasm" and "nucleus" were abundantly enriched. Molecular function, for the target proteins were mainly closely related to "enzyme binding" and "identical protein binding". A total of 74 pathways were obtained by KEGG pathway analysis (Table S4). After sorting according to the p-value, the top 10 signaling pathways were selected for mapping (Figure 3B). Matrine's anti-PRRSV targets were mainly concentrated in the "IL-17 signaling pathway" and "TNF signaling pathway". Finally, we prepared the Network and Type files that can define "matrine-core target-pathway", and input Cytoscape 3.7.3 software to build the network (Figure 4). The results of the network topology analysis showed that there were 21 network nodes, 59 network edges, 0.281 network densities, 4 network diameters, 2 network radii, 0.242 network centralizations, 0.413 network heterogeneity, 420 shortest paths, 1.981 lengths of the characteristic path, and the average number of neighbors were 5.619. The key targets screening criteria were set as Degree Un-Dir > 5.619. A total of 5 key targets were obtained, such as: CASP3, GSK3B, HSP90AB1,MAPK14 and MAPK8.

Molecular docking

Using AutoDockTools 1.5.6 software for molecular docking, the interaction and binding mode of target proteins and matrine can be explained at the molecular level. The matrine was docked into the active pocket of the protein and the theoretical binding mode was displayed using PyMOL software (Figure 5). The binding free energies of matrine to HSP90AB1 and HSPA8 were −8.52 kcal/mol and −5.47 kcal/mol, respectively (Figure 6). The results showed that matrine can bind tightly to HSP90AB1 and HSPA8.

Determination of mRNA/protein expression of HSPA8, HSP90AB1, and PRRSV N

After virus infection was compared with the cell control group, the expression of the *PRRSV N* gene was significantly increased ($p < 0.05$). The *PRRSV N* gene copies of MVH, MVM and MVL groups were significantly reduced compared to the virus control group ($p < 0.05$) (Figures 7A, 7D and 7G) with the prolonged incubation time of matrine and PRRSV, the mRNA expression of *HSPA8* and *HSP90AB1* in the virus control group gradually increased compared with the cell control group, and the difference was resulted significant ($p < 0.05$) compared with the virus control group, the mRNA expression of *HSPA8* and *HSP90AB1* in

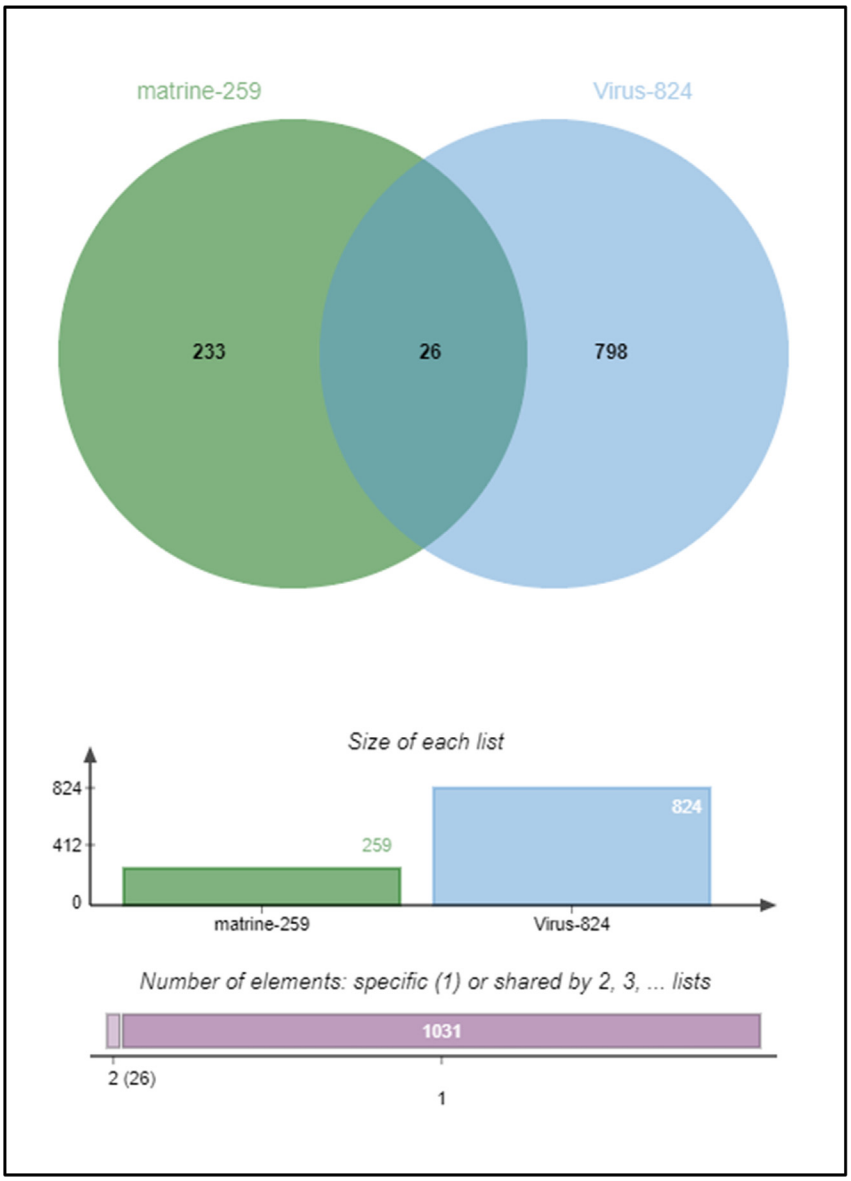

Figure 1. Intersection of matrine targets and disease targets related to porcine reproductive and respiratory syndrome

See also Tables S1 and S2.

each groups of MVH, MVM and MVL were significantly decreased ($p < 0.05$) (Figures 7B, 7C, 7E, 7F, 7H and 7I).

At different treatments period points, compared with the cell control group, the PRRSV N protein expression in the virus control group was significantly increased ($p < 0.05$), and there was a trend of increasing PRRSV N protein expression with the prolongation of treatment time. Compared with the virus control group, the expression of PRRSV N protein in each group of MVH, MVM and MVL were significantly decreased ($p < 0.05$), indicating that matrine can inhibit the replication of PRRSV. At 48 h and 72 h of treatment, the expression of HSPA8 and HSP90AB1 in MVH, MVM and MVL groups were significantly decreased compared with the virus control group, respectively ($p < 0.05$) (Figures 8B and 8C). The above results indicated that PRRSV infection of Marc-145 cells would encourage the expression of HSPA8 and HSP90AB1 to promote virus infection of cells. After matrine treatment, the expression of HSPA8 and HSP90AB1 proteins

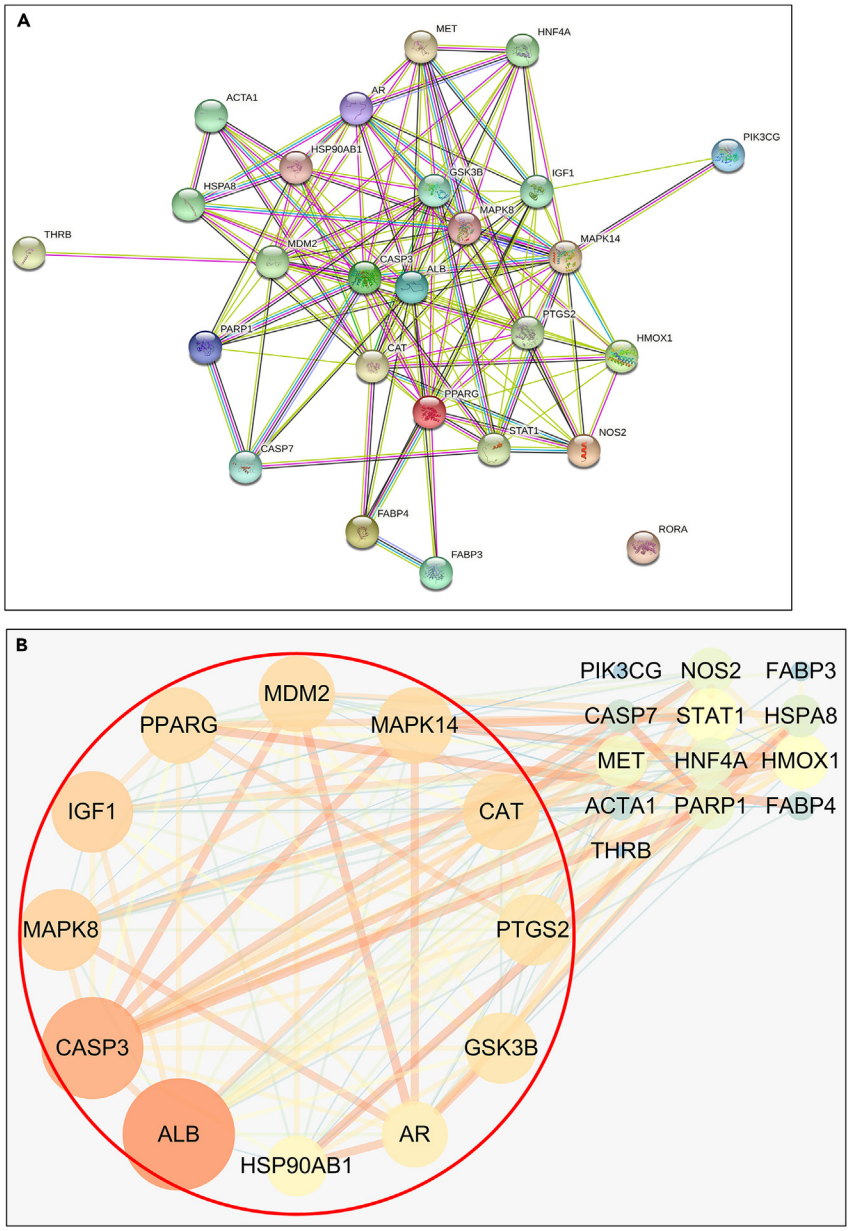

Figure 2. PPI network

(A) Protein interaction network diagram of 26 potential targets.

(B) The 12 core target proteins that have been screened, highlighted in the red box. The core target screening criteria were set as Degree Un-Dir >11.04.

were decreased, as compared to the expression of PRRSV N. Later, these confirmed the correlation between HSPA8, HSP90AB1, and matrine's anti-PRRSV effect on Marc-145 cells, respectively.

DISCUSSION

PRRS, which was caused by PRRSV infection, is an acute, contact animal infectious disease with high morbidity, high infectious rate, and high mortality. Owing to the immunosuppressive properties of PRRSV, the current antiviral therapy is ineffective, so it is of great significance to develop new and effective anti-PRRSV drugs.[10] Various earlier studies have shown that matrine can achieve the anti-PRRSV effect by directly inactivating the virus *in vitro* and interfering with PRRSV-induced apoptosis, but the target of matrine for its antiviral effect is not yet clear. Drugs and diseases are linked by targets screened by network

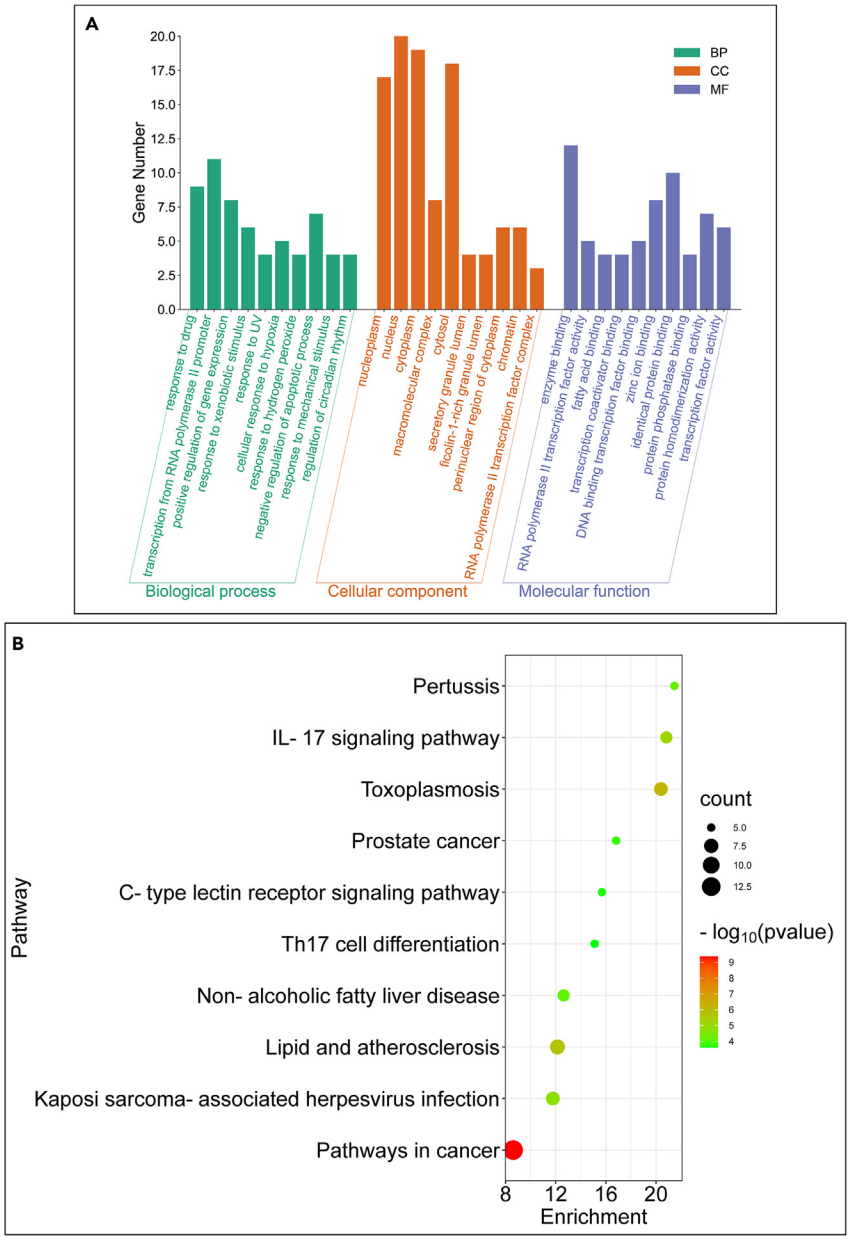

Figure 3. GO enrichment analysis and KEGG pathway analysis

(A) GO enrichment analysis.

(B) KEGG signal pathway analysis. The results of GO enrichment analysis and KEGG signal pathway analysis were arranged in ascending order of p value, and the top 10 objects were selected successively. All p-values were less than 0.01.

See also Tables S3 and S4.

pharmacology. The research on the targets of TCM action will be promoted by network pharmacology with massive biomedical data and continuously improving experimental techniques.[11] In this study, we have used network pharmacology and molecular docking to predict and screen the anti-PRRSV targets of matrine, and used matrine to treat PRRSV-infected Marc-145 cells to verify the reliability of the prediction.

The "PharmMapper database: https://www.lilab-ecust.cn/pharmmapper/" was founded on the pharmacophore to identify potential targets of a given drug or natural compound.[12] The "CTD: https://www.ctdbase.org" provides information on the interaction between chemical exposures, genes and proteins, phenotypes and diseases, and includes more than 7,212 diseases, including animal disease PRRS.[13] In this study,

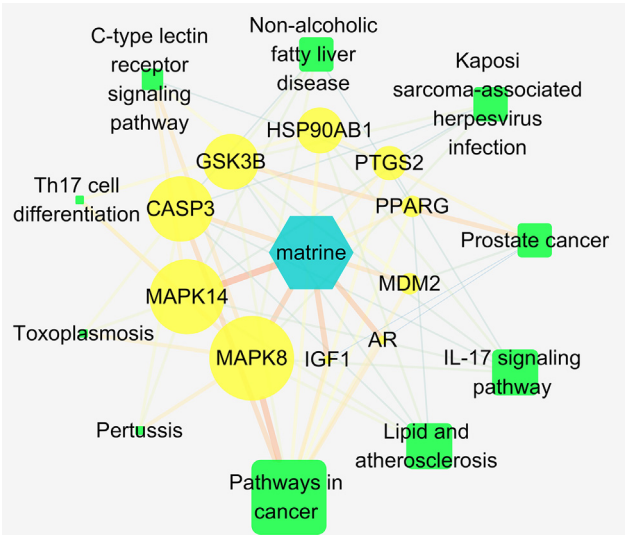

Figure 4. Network of "matrine-core target-pathway"

The blue, yellow and green color represent matrine, the core targets and the signal pathways, respectively. The key targets screening criteria were set as Degree Un-Dir > 5.619.

26 anti-PRRSV targets of matrine were discovered through network pharmacology. Through the construction of the PPI network, "matrine-core target-pathway" network, and molecular docking screening methods, HSPA8 and HSP90AB1 were determined as the final target proteins. Both HSPA8 and HSP90AB1 belong to the heat shock proteins (HSPs). HSPs are classes of proteins that are widely present

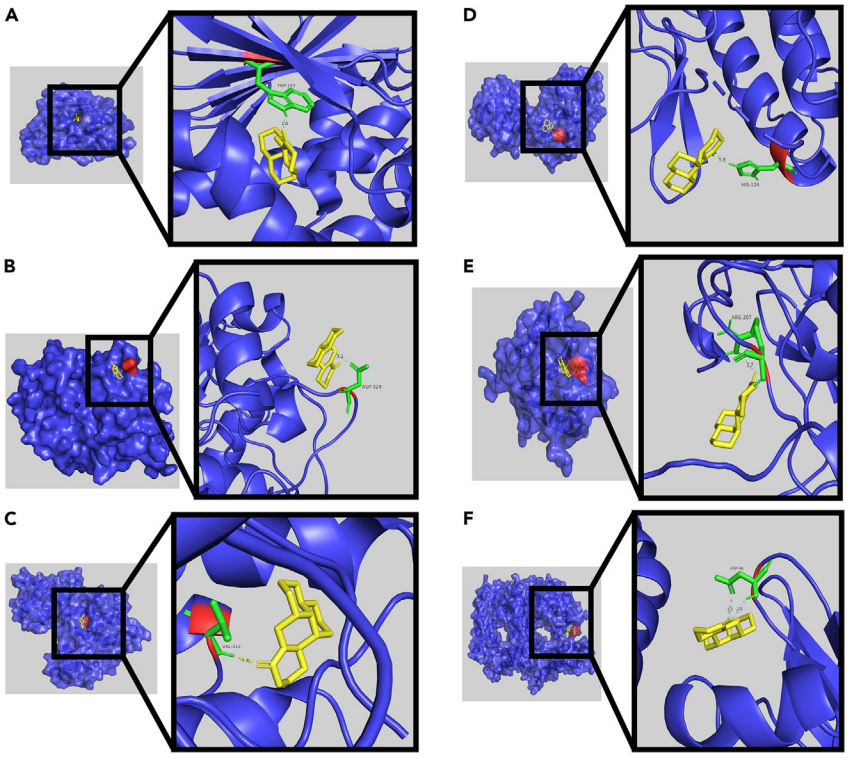

Figure 5. Schematic diagram of the interaction between matrine and target proteins

(A) HSP90AB1, (B) GSK3B, (C) MAPK8, (D) MAPK14, (E) CASP3, (F) HSPA8. Molecular docking is done by AutodockTools.

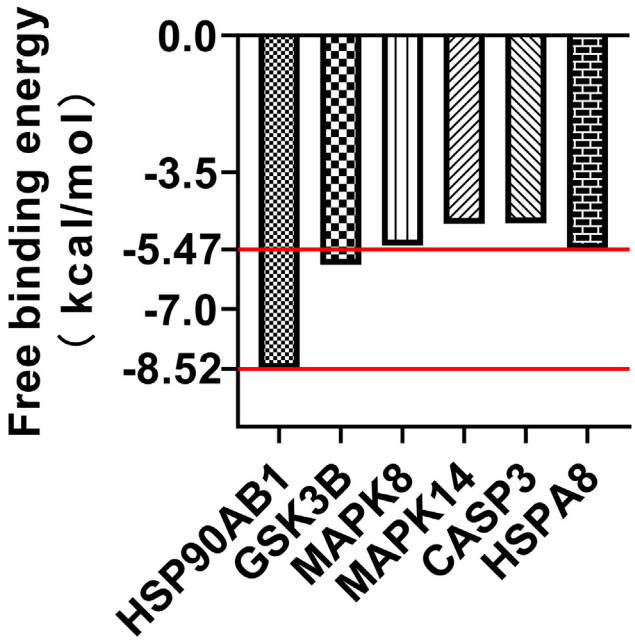

Figure 6. Summary of docking free binding energy

in both prokaryotes and in eukaryotes and are highly evolutionarily conserved.[14] According to the molecular weight of the protein, it can be divided into HSP90, HSP70, HSP60, and HSP40. HSPs are mainly involved in the folding of newly synthesized polypeptides and proteins in cells, assisting in the assembly of proteins and complexes, and the degradation of misfolded proteins.[15] The protein HSPA8 not only has the physiological function of a molecular chaperone, but also widely participates in regulating the life cycle of various viruses.[16] HSP70 and HSPA8 are key components of dengue virus (DENV) invading C6/36 cells.[17] During PRRSV invasion of Marc-145 cells, HSPA8 interacts with PRRSV GP4 to mediate PRRSV adhesion and internalization through clathrin-dependent endocytosis (CME).[18] In addition, heat stress can antagonize the inhibition of PRRSV replication caused by HSP70 inhibitors.[19]

HSP90 plays an important role in the folding, maturation and activation of client proteins to maintain the homeostasis of the intracellular environment.[20] In addition, HSP90 can also promote viral infection by stabilizing viral proteins against their degradation by the ubiquitin-proteasome pathway or by autophagy-mediated degradation pathways.[21] Li et al. reported that HSP90AB1 is a class of molecular chaperones necessary to maintain MERS-CoV nucleoprotein stability.[22] In HSP90AB1 gene knockout experiments, it was found that HSP90AB1 is involved in the immune and inflammatory responses of porcine-delta coronavirus (PDCoV) infected 293 T cells.[23] Li et al. have discovered the mechanism by which encephalon myocarditis virus (EMCV) utilizes HSP90AB1 to promote viral proliferation: EMCV VP2 hijacks HSP90AB1 to induce upregulation of HSP90AB1 expression to inhibit the activation of IFN-β signaling pathway.[24]

In addition to the research that HSPA8 and HSP90AB1 are involved in the viral life process alone, researchers also pay attention to the viral infection process that they both participate in. HSPA8 and HSP90AB1 are jointly involved in the infection process of the human enterovirus 71 (EV-71), and HSPA8 is involved in the assembly and release of progeny viruses.[25] HSP90AB1 inhibitors can reduce the stability of EV-71 capsid protein and affect the infectivity of the virus.[26] HSP70 and HSP90 can act as receptor complexes of macrophages to participate in the invasion of the dengue virus (DENV). Heat stress-induced upregulation of HSP70 and HSP90 can promote the invasion of the virus.[27] After treatment with inhibitors, the viral load can be significantly reduced.[28] HSPA8 and HSP90 can form a complex with the non-structural protein 5A of the hepatitis C virus (HCV) to affect the replication of the virus. Inhibiting the formation of the complex will affect the assembly of the progeny virus and inhibit the replication of HCV.[29,30]

All of the above studies have demonstrated that HSPA8 and HSP90AB1, individually or together, are extensively involved in different stages of the life cycle of various viruses. In this study, the changes in HSPA8 and

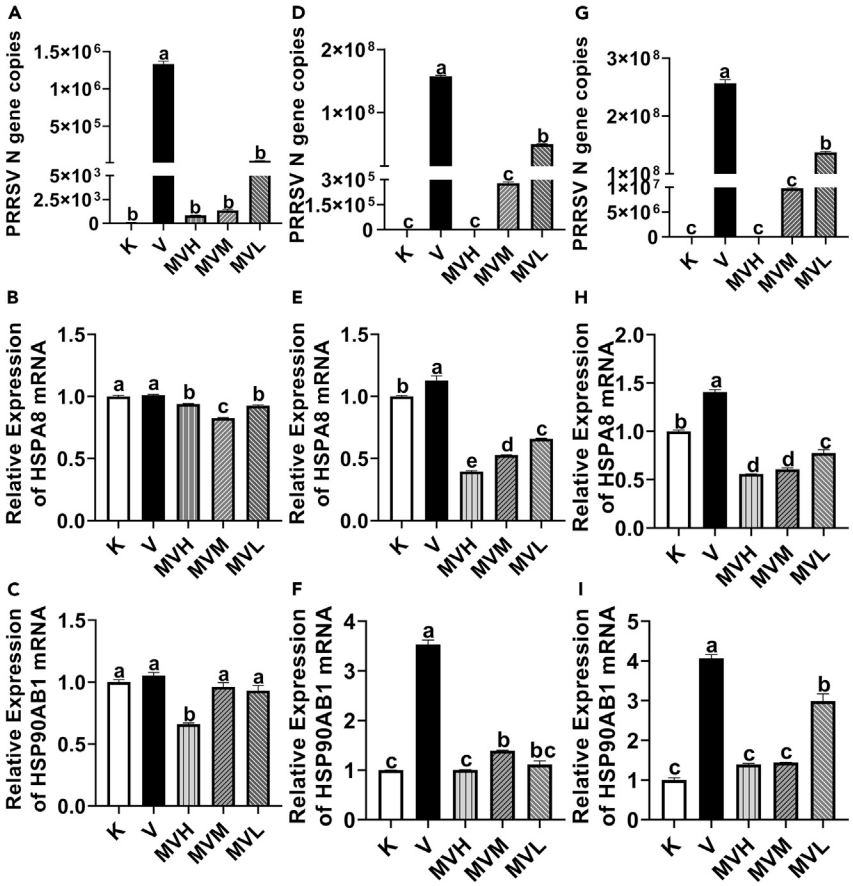

Figure 7. The expression of *PRRSV N, HSPA8* and *HSP90AB1* mRNA in Marc-145 cells treated with different treatments

Effects of high, middle and low doses of matrine on the expression of *PRRSV N*, *HSPA8* and *HSP90AB1* mRNA in Marc-145 infected with PRRSV for 24 h (A, B, C), 48 h (D, E, F) and 72 h (G, H, I). All data were expressed as mean ± standard errors of the mean (mean ± SEM), where n represented the number of groups in the experiment and n = 5. "a, b, c, d, e" represented a significant difference between different columns ($p < 0.05$).

HSP90AB1 mRNA and proteins were detected by qRT-PCR and western blot. From the present study, the results showed that compared with the cell control group, the expression of HSPA8 and HSP90AB1 mRNA and proteins were significantly increased by virus infection. After treatment with matrine, the expressions of HSPA8 and HSP90AB1 were significantly decreased with the prolongation of treatment time, indicating that HSPA8 and HSP90AB1 are closely related to matrine's anti-PRRSV effect. The findings remind researchers that heat shock proteins, ancient and evolutionarily conserved proteins, should be re-examined not only for their important role in intracellular homeostasis, but also for their close connection with the viral life cycle. This reflects the potential of HSPs as targets for antiviral drugs.

Limitations of the study

In this work, the prediction results of the potential targets of matrine are limited by the contents included in the database. With the deepening of the research on the targets of matrine, the prediction results of network pharmacology are expected to be more accurate. In this study, the application of the Marc-145 cell model infected with PRRSV was a convenient method of study, but the application of porcine alveolar macrophages (PAMs) was necessary for an in-depth study.

STAR★METHODS

Detailed methods are provided in the online version of this paper and include the following:

- KEY RESOURCES TABLE

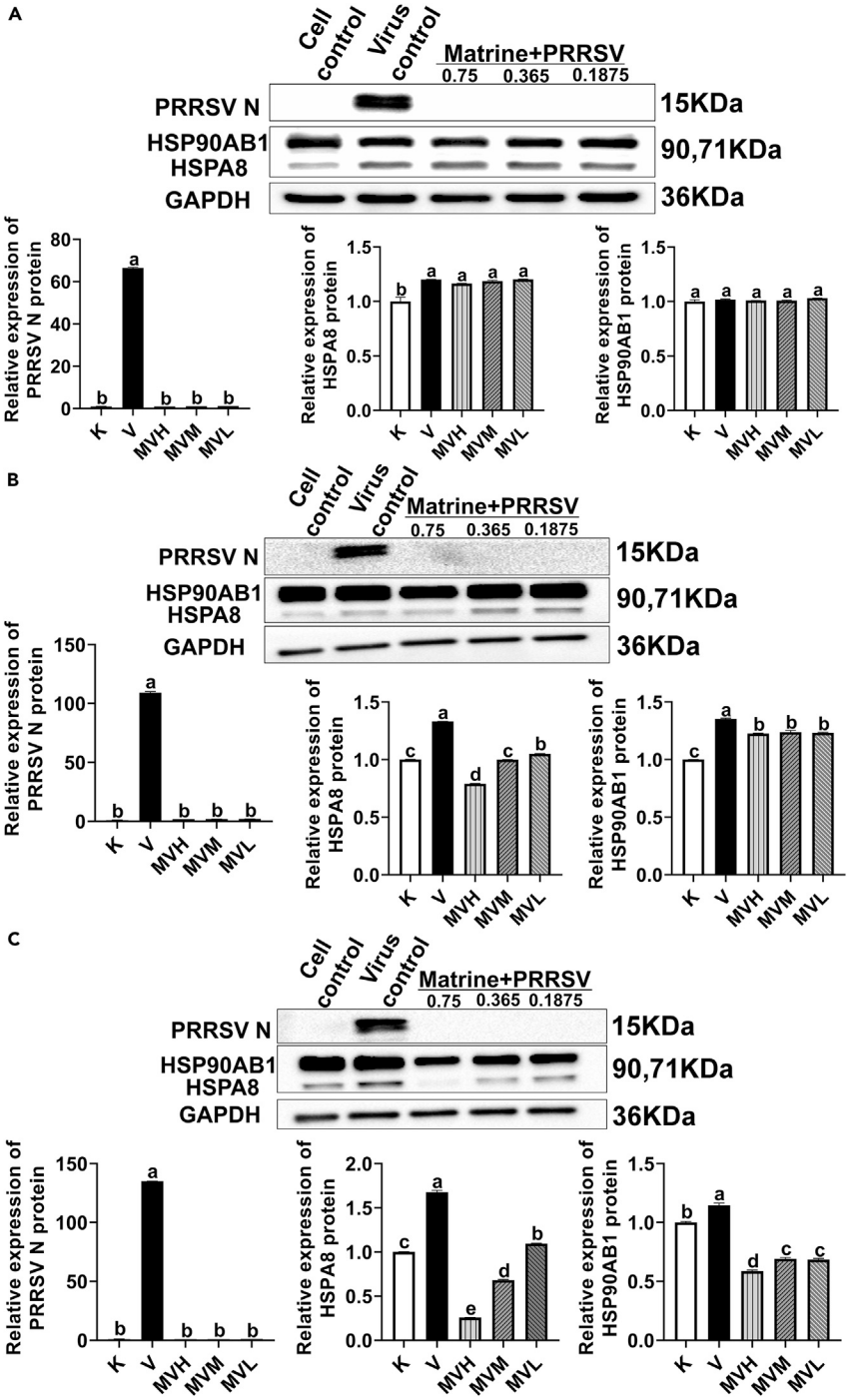

Figure 8. Expression levels of PRRSV N, HSPA8 and HSP90AB1 after Marc-145 infection with PRRSV at different time points

(A) 24 h, (B) 48 h and (C) 72 h. All data were expressed as mean ± standard errors of the mean (mean ± SEM), where n represented the number of groups in the experiment and n = 5. "a, b, c, d, e" represented a significant difference between different columns ($p < 0.05$).

- RESOURCE AVAILABILITY
  - Lead contact
  - Materials availability

- Data and code availability
- EXPERIMENTAL MODEL AND SUBJECT DETAILS
  - Cell culture
- METHOD DETAILS
  - Anti-PRRSV targets of matrine
  - PPI network
  - GO and KEGG pathway analysis
  - Molecular docking
  - Construct experimental model
  - qRT-PCR
  - Western blot analysis
- QUANTIFICATION AND STATISTICAL ANALYSIS

SUPPLEMENTAL INFORMATION

Supplemental information can be found online at https://doi.org/10.1016/j.isci.2023.106371.

ACKNOWLEDGMENTS

This work was supported by National Natural Science Foundation of China (Grant No. 32172904); the special fund for Science and Technology Innovation Teams of Shanxi Province (202204051001021); Scientific and Technological Innovation Programs of Higher Education Institutions in Shanxi (Grant No. 2021L108); Key Research and Development Plan of Shanxi Province (Grant No. 202102140601019); Shanxi "1331 Project" (No. 20211331-16, No. 20211331-13); Innovation Projects of College of Veterinary Medicine, Shanxi Agricultural University (DY-M003) and the earmarked Fund for Modern Agro-industry Technology Research System.

Thanks to Figdraw (https://www.figdraw.com/static/index.html) for providing drawing help for the Graphical Abstract part of this article. Thanks to online data analysis website (http://www.bioinformatics.com.cn/) for its help in the enrichment analysis and visualization of the data in this study.

AUTHOR CONTRIBUTIONS

Conceptualization, N.S., H.L., Y.Z., X.L., H.Z., P.S., Y.S., W.Y., K.F., H.Y., J.Z., Z.Z., and J.W.; Investigation, N.S. and H.L.; Writing – Original Draft, Y.Z.; Writing – Review and Editing, N.S., H.L., and Y.Z.; Funding Acquisition, N.S. and H.L.; Supervision, N.S. and H.L.

DECLARATION OF INTERESTS

The authors declare no competing interests.

INCLUSION AND DIVERSITY

We support inclusive, diverse, and equitable conduct of research.

Received: September 30, 2022
Revised: December 8, 2022
Accepted: March 6, 2023
Published: March 10, 2023

REFERENCES

1. Wensvoort, G., Terpstra, C., Pol, J.M., ter Laak, E.A., Bloemraad, M., de Kluyver, E.P., Kragten, C., van Buiten, L., den Besten, A., Wagenaar, F., et al. (1991). Mystery swine disease in The Netherlands: the isolation of Lelystad virus. Vet. Q. *13*, 121–130. https://doi.org/10.1080/01652176.1991.9694296.

2. Wensvoort, G., de Kluyver, E.P., Pol, J.M., Wagenaar, F., Moormann, R.J., Hulst, M.M., Bloemraad, R., den Besten, A., Zetstra, T., and Terpstra, C. (1992). Lelystad virus, the cause of porcine epidemic abortion and respiratory syndrome: a review of mystery swine disease research at Lelystad. Vet. Microbiol. *33*, 185–193. https://doi.org/10.1016/0378-1135(92)90046-v.

3. Li, B., Fang, L., Guo, X., Gao, J., Song, T., Bi, J., He, K., Chen, H., and Xiao, S. (2011). Epidemiology and evolutionary characteristics of the porcine reproductive and respiratory syndrome virus in China between 2006 and 2010. J. Clin. Microbiol. *49*, 3175–3183. https://doi.org/10.1128/JCM.00234-11.

4. Zhou, L., Wang, Z., Ding, Y., Ge, X., Guo, X., and Yang, H. (2015). NADC30-like strain of porcine reproductive and respiratory syndrome virus, China. Emerg. Infect. Dis. *21*, 2256–2257. https://doi.org/10.3201/eid2112.150360.

5. Fang, K., Liu, S., Li, X., Chen, H., and Qian, P. (2022). Epidemiological and genetic characteristics of porcine reproductive and

respiratory syndrome virus in South China between 2017 and 2021. Front. Vet. Sci. *9*, 853044. https://doi.org/10.3389/fvets.2022.853044.

6. Renukaradhya, G.J., Meng, X.J., Calvert, J.G., Roof, M., and Lager, K.M. (2015). Live porcine reproductive and respiratory syndrome virus vaccines: current status and future direction. Vaccine *33*, 4069–4080. https://doi.org/10.1016/j.vaccine.2015.06.092.

7. Chakravarti, R., Singh, R., Ghosh, A., Dey, D., Sharma, P., Velayutham, R., Roy, S., and Ghosh, D. (2021). A review on potential of natural products in the management of COVID-19. RSC Adv. *11*, 16711–16735. https://doi.org/10.1039/d1ra00644d.

8. Musarra-Pizzo, M., Pennisi, R., Ben-Amor, I., Mandalari, G., and Sciortino, M.T. (2021). Antiviral activity exerted by natural products against human viruses. Viruses *13*, 828. https://doi.org/10.3390/v13050828.

9. Sun, N., Wang, Z.W., Wu, C.H., Li, E., He, J.P., Wang, S.Y., Hu, Y.L., Lei, H.M., and Li, H.Q. (2014). Antiviral activity and underlying molecular mechanisms of Matrine against porcine reproductive and respiratory syndrome virus in vitro. Res. Vet. Sci. *96*, 323–327. https://doi.org/10.1016/j.rvsc.2013.12.009.

10. Guo, Z., Chen, X.X., Li, R., Qiao, S., and Zhang, G. (2018). The prevalent status and genetic diversity of porcine reproductive and respiratory syndrome virus in China: a molecular epidemiological perspective. Virol. J. *15*, 2. https://doi.org/10.1186/s12985-017-0910-6.

11. Yuan, Z., Pan, Y., Leng, T., Chu, Y., Zhang, H., Ma, J., and Ma, X. (2022). Progress and prospects of research ideas and methods in the network pharmacology of traditional Chinese medicine. J. Pharm. Pharm. Sci. *25*, 218–226. https://doi.org/10.18433/jpps32911.

12. Wang, X., Shen, Y., Wang, S., Li, S., Zhang, W., Liu, X., Lai, L., Pei, J., and Li, H. (2017). PharmMapper 2017 update: a web server for potential drug target identification with a comprehensive target pharmacophore database. Nucleic Acids Res. *45*, W356–W360. https://doi.org/10.1093/nar/gkx374.

13. Davis, A.P., Grondin, C.J., Johnson, R.J., Sciaky, D., McMorran, R., Wiegers, J., Wiegers, T.C., and Mattingly, C.J. (2019). The comparative Toxicogenomics database: update 2019. Nucleic Acids Res. *47*, D948–D954. https://doi.org/10.1093/nar/gky868.

14. Balch, W.E., Morimoto, R.I., Dillin, A., and Kelly, J.W. (2008). Adapting proteostasis for disease intervention. Science *319*, 916–919. https://doi.org/10.1126/science.1141448.

15. Hu, C., Yang, J., Qi, Z., Wu, H., Wang, B., Zou, F., Mei, H., Liu, J., Wang, W., and Liu, Q. (2022). Heat shock proteins: biological functions, pathological roles, and therapeutic opportunities. MedComm *3*, e161. https://doi.org/10.1002/mco2.161.

16. Wang, Z., Li, Y., Yang, X., Zhao, J., Cheng, Y., and Wang, J. (2020). Mechanism and complex roles of HSC70 in viral infections. Front. Microbiol. *11*, 1577. https://doi.org/10.3389/fmicb.2020.01577.

17. Vega-Almeida, T.O., Salas-Benito, M., De Nova-Ocampo, M.A., Del Angel, R.M., and Salas-Benito, J.S. (2013). Surface proteins of C6/36 cells involved in dengue virus 4 binding and entry. Arch. Virol. *158*, 1189–1207. https://doi.org/10.1007/s00705-012-1596-0.

18. Wang, L., Li, R., Geng, R., Zhang, L., Chen, X.X., Qiao, S., and Zhang, G. (2022). Heat shock protein member 8 (HSPA8) is involved in porcine reproductive and respiratory syndrome virus attachment and internalization. Microbiol. Spectr. *10*, e0186021. https://doi.org/10.1128/spectrum.01860-21.

19. Gao, J., Xiao, S., Liu, X., Wang, L., Ji, Q., Mo, D., and Chen, Y. (2014). Inhibition of HSP70 reduces porcine reproductive and respiratory syndrome virus replication in vitro. BMC Microbiol. *14*, 64. https://doi.org/10.1186/1471-2180-14-64.

20. Hoter, A., El-Sabban, M.E., and Naim, H.Y. (2018). The HSP90 family: structure, regulation, function, and implications in health and disease. Int. J. Mol. Sci. *19*, 2560. https://doi.org/10.3390/ijms19092560.

21. Wang, Y., Jin, F., Wang, R., Li, F., Wu, Y., Kitazato, K., and Wang, Y. (2017). HSP90: a promising broad-spectrum antiviral drug target. Arch. Virol. *162*, 3269–3282. https://doi.org/10.1007/s00705-017-3511-1.

22. Li, C., Chu, H., Liu, X., Chiu, M.C., Zhao, X., Wang, D., Wei, Y., Hou, Y., Shuai, H., Cai, J., et al. (2020). Human coronavirus dependency on host heat shock protein 90 reveals an antiviral target. Emerg. Microbes Infect. *9*, 2663–2672. https://doi.org/10.1080/22221751.2020.1850183.

23. Zhao, Y., Chen, R., Xiao, D., Zhang, L., Song, D., Wen, Y., Wu, R., Zhao, Q., Du, S., Wen, X., et al. (2022). A comparative transcriptomic analysis reveals that HSP90AB1 is involved in the immune and inflammatory responses to porcine deltacoronavirus infection. Int. J. Mol. Sci. *23*, 3280. https://doi.org/10.3390/ijms23063280.

24. Li, Q., Li, X., Wu, B., Niu, Y., Ma, R., Xie, J., Ali, A., and Feng, R. (2021). Host protein, HSP90beta, antagonizes IFN-beta signaling pathway and facilitates the proliferation of encephalomyocarditis virus in vitro. Virus Res. *305*, 198547. https://doi.org/10.1016/j.virusres.2021.198547.

25. Su, Y.S., Hsieh, P.Y., Li, J.S., Pao, Y.H., Chen, C.J., and Hwang, L.H. (2020). The heat shock protein 70 family of chaperones regulates all phases of the enterovirus A71 life cycle. Front. Microbiol. *11*, 1656. https://doi.org/10.3389/fmicb.2020.01656.

26. Tsou, Y.L., Lin, Y.W., Chang, H.W., Lin, H.Y., Shao, H.Y., Yu, S.L., Liu, C.C., Chitra, E., Sia, C., and Chow, Y.H. (2013). Heat shock protein 90: role in enterovirus 71 entry and assembly and potential target for therapy. PLoS One *8*, e77133. https://doi.org/10.1371/journal.pone.0077133.

27. Reyes-Del Valle, J., Chávez-Salinas, S., Medina, F., and Del Angel, R.M. (2005). Heat shock protein 90 and heat shock protein 70 are components of dengue virus receptor complex in human cells. J. Virol. *79*, 4557–4567. https://doi.org/10.1128/JVI.79.8.4557-4567.2005.

28. Taguwa, S., Maringer, K., Li, X., Bernal-Rubio, D., Rauch, J.N., Gestwicki, J.E., Andino, R., Fernandez-Sesma, A., and Frydman, J. (2015). Defining Hsp70 subnetworks in dengue virus replication reveals key vulnerability in flavivirus infection. Cell *163*, 1108–1123. https://doi.org/10.1016/j.cell.2015.10.046.

29. Khachatoorian, R., Ganapathy, E., Ahmadieh, Y., Wheatley, N., Sundberg, C., Jung, C.L., Arumugaswami, V., Raychaudhuri, S., Dasgupta, A., and French, S.W. (2014). The NS5A-binding heat shock proteins HSC70 and HSP70 play distinct roles in the hepatitis C viral life cycle. Virology *454–455*, 118–127. https://doi.org/10.1016/j.virol.2014.02.016.

30. Kim, M.G., Moon, J.S., Kim, E.J., Lee, S.H., and Oh, J.W. (2012). Destabilization of PDK1 by Hsp90 inactivation suppresses hepatitis C virus replication through inhibition of PRK2-mediated viral RNA polymerase phosphorylation. Biochem. Biophys. Res. Commun. *421*, 112–118. https://doi.org/10.1016/j.bbrc.2012.03.126.

31. Zhang, H., Cao, Z., Sun, P., Khan, A., Guo, J., Sun, Y., Yu, X., Fan, K., Yin, W., Li, E., et al. (2022). A novel strategy for optimal component formula of anti-PRRSV from natural compounds using tandem mass tag labeled proteomic analyses. BMC Vet. Res. *18*, 179. https://doi.org/10.1186/s12917-022-03184-w.

32. Burley, S.K., Bhikadiya, C., Bi, C., Bittrich, S., Chen, L., Crichlow, G.V., Christie, C.H., Dalenberg, K., Di Costanzo, L., Duarte, J.M., et al. (2021). RCSB Protein Data Bank: powerful new tools for exploring 3D structures of biological macromolecules for basic and applied research and education in fundamental biology, biomedicine, biotechnology, bioengineering and energy sciences. Nucleic Acids Res. *49*, D437–D451. https://doi.org/10.1093/nar/gkaa1038.

33. UniProt Consortium, Martin, M.-J., Orchard, S., Magrane, M., Ahmad, S., Alpi, E., Bowler-Barnett, E.H., Britto, R., Bye-A-Jee, H., Cukura, A., et al. (2023). UniProt: the universal protein knowledgebase in 2023. Nucleic Acids Res. *51*, D523–D531. https://doi.org/10.1093/nar/gkac1052.

34. Kim, S., Chen, J., Cheng, T., Gindulyte, A., He, J., He, S., Li, Q., Shoemaker, B.A., Thiessen, P.A., Yu, B., et al. (2023). PubChem 2023 update. Nucleic Acids Res. *51*, D1373–D1380. https://doi.org/10.1093/nar/gkac956.

35. Szklarczyk, D., Kirsch, R., Koutrouli, M., Nastou, K., Mehryary, F., Hachilif, R., Gable, A.L., Fang, T., Doncheva, N.T., Pyysalo, S., et al. (2023). The STRING database in 2023: protein-protein association networks and functional enrichment analyses for any sequenced genome of interest. Nucleic Acids

Res. *51*, D638–D646. https://doi.org/10.1093/nar/gkac1000.

36. Sherman, B.T., Hao, M., Qiu, J., Jiao, X., Baseler, M.W., Lane, H.C., Imamichi, T., and Chang, W. (2022). DAVID: a web server for functional enrichment analysis and functional annotation of gene lists (2021 update). Nucleic Acids Res. *50*, W216–W221. https://doi.org/10.1093/nar/gkac194.

37. Shannon, P., Markiel, A., Ozier, O., Baliga, N.S., Wang, J.T., Ramage, D., Amin, N., Schwikowski, B., and Ideker, T. (2003). Cytoscape: a software environment for integrated models of biomolecular interaction networks. Genome Res. *13*, 2498–2504. https://doi.org/10.1101/gr.1239303.

38. Österberg, F., Morris, G.M., Sanner, M.F., Olson, A.J., and Goodsell, D.S. (2002). Automated docking to multiple target structures: incorporation of protein mobility and structural water heterogeneity in AutoDock. Proteins *46*, 34–40. https://doi.org/10.1002/prot.10028.

39. Lill, M.A., and Danielson, M.L. (2011). Computer-aided drug design platform using PyMOL. J. Comput. Aided Mol. Des. *25*, 13–19. https://doi.org/10.1007/s10822-010-9395-8.

40. Feeney, B., Pop, C., Swartz, P., Mattos, C., and Clark, A.C. (2006). Role of loop bundle hydrogen bonds in the maturation and activity of (Pro)caspase-3. Biochemistry *45*, 13249–13263. https://doi.org/10.1021/bi0611964.

41. Yang, J., Cron, P., Good, V.M., Thompson, V., Hemmings, B.A., and Barford, D. (2002). Crystal structure of an activated Akt/Protein Kinase B ternary complex with GSK3-peptide and AMP-PNP. Nat. Struct. Biol. *9*, 940–944. https://doi.org/10.1038/nsb870.

42. Huck, J.D., Que, N.L.S., Sharma, S., Taldone, T., Chiosis, G., and Gewirth, D.T. (2019). Structures of Hsp90α and Hsp90β bound to a purine-scaffold inhibitor reveal an exploitable residue for drug selectivity. Proteins *87*, 869–877. https://doi.org/10.1002/prot.25750.

43. Garai, Á., Zeke, A., Gógl, G., Törő, I., Fördős, F., Blankenburg, H., Bárkai, T., Varga, J., Alexa, A., Emig, D., et al. (2012). Specificity of linear motifs that bind to a common mitogen-activated protein kinase docking groove. Sci. Signal. *5*, ra74. https://doi.org/10.1126/scisignal.2003004.

44. Jones, A.M., Westwood, I.M., Osborne, J.D., Matthews, T.P., Cheeseman, M.D., Rowlands, M.G., Jeganathan, F., Burke, R., Lee, D., Kadi, N., et al. (2016). A fragment-based approach applied to a highly flexible target: insights and challenges towards the inhibition of HSP70 isoforms. Sci. Rep. *6*, 34701. https://doi.org/10.1038/srep34701.

45. Diskin, R., Lebendiker, M., Engelberg, D., and Livnah, O. (2007). Structures of p38α active mutants reveal conformational changes in L16 loop that induce autophosphorylation and activation. J. Mol. Biol. *365*, 66–76. https://doi.org/10.1016/j.jmb.2006.08.043.

STAR★METHODS

KEY RESOURCES TABLE

REAGENT or RESOURCE	SOURCE	IDENTIFIER
Antibodies		
Mouse monoclonal anti-GAPDH	Proteintech Group	RRID: AB_2107436
Rabbit polyclonal anti-HSPA8	ABclonal	Cat#A14001; RRID: AB_2313773
Rabbit monoclonal anti-HSP90 beta	Abcom	Cat#ab203085; RRID: AB2313773
Mouse monoclonal anti-PRRSV N	LVDU	Cat#LD062; RRID: AB2313773
Goat anti-Mouse HRP-conjugated Antibody	Bioss	Cat#bs-0293G; RRID: AB2313773
Goat anti-Rabbit HRP-conjugated Antibody	Bioss	Cat#bs-0295G; RRID: AB2313773
Bacterial and virus strains		
Porcine reproductive and respiratory syndrome virus (PRRSV)	Isolated from one suspected PRRSV infected piglet by our lab.[31]	N/A
Chemicals, peptides, and recombinant proteins		
Matrine	National Institutes for Food and Drug Control	Cat#110805-201709
Critical commercial assays		
Trizol	TaKaRa	Cat#SD1412
Prime Script ™ RT reagent Kit with gDNA Eraser	TaKaRa	Cat#RR047A
2×SYBR Green Low ROX qPCR Master Mix	Bimake	Cat#B21702
RIPA buffer	Solarbio	Cat#R0010
Phosphatase Inhibitor	Bimake	Cat#B15001
BCA protein concentration assay kit	Beyotime	Cat#P0009
4×LDS Sample Buffer	Invitrogen	Cat#NP0008
SDS-PAGE gel preparation kit	Boster	Cat#AR0138
uper-sensitive ECL ready-to-use substance kit	Boster	Cat#AR1173
Deposited data		
RCSB PDB	Burley et al.[32]	https://www.rcsb.org
Uniprot	Bateman et al.[33]	https://www.uniprot.org
Comparative Toxicogenomics Database	Davis et al.[13]	https://www.ctdbase.org
PharmMapper	Wang et al.[12]	https://www.lilab-ecust.cn/pharmmapper/
PubChem	Kim et al.[34]	https://pubchem.ncbi.nlm.nih.gov
STRING	Szklarczyk et al.[35]	https://cn.string-db.org
DAVID	Sherman et al.[36]	https://david.ncifcrf.gov
Experimental models: Cell lines		
Monkey Embryonic Kidney Epithelial Cells	China Institute of Veterinary Drug Control	N/A
Oligonucleotides		
Primer: GAPDH Forward	This paper	5′GTCAGTGGTGGACCTGACCT-3′
Primer: GAPDH Reverse	This paper	5′TGCTGTAGCCAAATTCGTTG-3′
Primer: HSPA8 Forward	This paper	5′CCCCATCATCACCAAGCTGT-3′
Primer: HSPA8 Reverse	This paper	5′CTCCACCACCAGGAAATCCC-3′
Primer: HSP90AB1 Forward	This paper	5′CATCCCCAACCCTCAGGAAC-3′

(*Continued on next page*)

Continued

REAGENT or RESOURCE	SOURCE	IDENTIFIER
Primer: HSP90AB1 Reverse	This paper	5′CAGCAGAAGACTCCCAAGCA-3′
Primer: PRRSV N Forward	This paper	5′AGAAGCCCCATTTCCCTCTA-3′
Primer: PRRSV N Reverse	This paper	5′CGGATCAGACGCACAGTATG-3′
Software and algorithms		
Cytoscape Version: 3.7.2	Shannon et al.[37]	https://cytoscape.org
AutoDockTools Version: 1.5.6	Österberg et al.[38]	https://autodock.scripps.edu
PyMol Version: 2.5.2	Lill et al.[39]	https://pymol.org/2/

RESOURCE AVAILABILITY

Lead contact

Further information and requests for resources and reagents should be directed to and will be fulfilled by the lead contact, Na Sun (snzh060511@126.com).

Materials availability

This study did not generate new unique reagents.

Data and code availability

- All data reported in this paper will be shared by the lead contact upon request.
- This paper does not report original code.
- Any additional information required to reanalyze the data reported in this paper is available from the lead contact upon request.

EXPERIMENTAL MODEL AND SUBJECT DETAILS

Cell culture

Monkey Embryonic Kidney Epithelial Cells (Marc-145) was purchased from China Institute of Veterinary Drug Control (China) cultured with Dulbecco's Modified Eagle Medium (DMEM) (Hyclone, USA) at 37°C and 5% CO_2. Matrine (110805-201709) was purchased from National Institutes for Food and Drug Control (China) and the purity was 98.7% detected by HPLC; PRRSV was amplified and preserved by our laboratory, and the virus titer of $10^{7.45}TCID_{50}$/mL was determined by the Reed-Muench method on Marc-145 cells and $10^{5.45}TCID_{50}$/mL PRRSV were used in this experiment.[31]

METHOD DETAILS

Anti-PRRSV targets of matrine

The 3D Conformer SDF file of the chemical structure of matrine was obtained from the "PubChem database[34] : https://pubchem.ncbi.nlm.nih.gov/" upload the SDF file of matrine and keep the default options of the "PharmMapper database: http://www.lilab-ecust.cn/pharmmapper/". Then the top 300 drug targets with the highest scores can be obtained. And the target gene was annotated by the "UniProt database[33]: http://www.uniprot.org/". In the :CTD: https://ctdbase.org/", "porcine reproductive and respiratory syndrome" was used as the keyword to search for relevant disease targets. Finally, the anti-PRRSV targets of matrine can be obtained after the intersection of the drug and the disease targets.

PPI network

Import matrine anti-PRRSV targets into the "String database[35]: https://string-db.org/" to obtain PPI and TSV files. Open the TSV file by Cytoscape 3.7.2 software[37] to generate a protein interaction network, and perform topological analysis on the network to obtain core targets.

GO and KEGG pathway analysis

The anti-PRRSV targets of matrine were imported into the "DAVID database[36]: https://david.ncifcrf.gov/" for GO and KEGG pathways analysis. The analysis results were sorted in descending order according to the

number of participating genes, the significance level was set to $p < 0.05$, and the top 10 analysis results were plotted respectively. Finally, the "matrine-core target-pathway" network was constructed using Cytoscape 3.7.2 software, to obtain key targets.

Molecular docking

Open the 3D Conformer SDF file of matrine with AutoDockTools 1.5.6,[38] delete water molecules, add hydrogen atoms and charge were in turn, describe it as a ligand and save it as a pdbqt file. The 3D structure pdb files of CAPS3 "PDB: 2J32[40]", GSK3B "PDB: 1O6L[41]", HSP90AB1 "PDB: 6N8Y[42]", MAPK8 "PDB: 2XRW[43]", HSPA8 "PDB: 5AQM[44]", and MAPK14 "PDB: 2FST[45]" obtained from the "RCSB Protein Data Bank[32]: https://www.rcsb.org/" were opened with AutoDockTools 1.5.6, and their structures were edited and defined as receptors and saved as pdbqt files. The semi-flexible docking method was used to dock the ligand and receptor, selected the conformation with the lowest docking binding energy for output and analysis, and finally use PyMol software[39] to generate the image.

Construct experimental model

For medium exchange treatment of monolayer Marc-145 cells grown in 6-well plates, add the culture medium of different treatment groups: Cell control / K (2% DMEM), Virus control / V (2% DMEM supplemented with PRRSV), MVH (2% DMEM supplemented with PRRSV+0.75 mg/mL MT), MVM (2% DMEM supplemented with PRRSV+0.365 mg/mL MT), and MVL (2% DMEM supplemented with PRRSV+0.1875 mg/mL MT). After 24 h, 48 h, and 72 h incubation with matrine and PRRSV, Marc-145 from all groups were collected RNA and protein were extracted to determine the HSPA8 HSP90AB1 and PRRSV N mRNA / protein expression.

qRT-PCR

Total RNA was extracted from Marc-145 cells according to the Trizol instruction manual, and then cDNA was synthesized using Prime Script ™ RT reagent Kit with gDNA Eraser. Set up qRT-PCR reactions using SYBR Green Low ROX qPCR Master Mix. A standard curve was generated using serially tenfold diluted plasmid containing and *PRRSV N* gene and the mRNA expression of *GAPDH* was used as a relative reference for each experiment.

Western blot analysis

Collected and washed the cells of each treatment groups with PBS, fully lyse the cells with RIPA buffer supplemented with 1% protease inhibitor and 1% phosphatase inhibitor, vortex and centrifuge to collect the supernatant, which was the total cell protein. After measuring the protein concentration using the BCA protein concentration assay kit, and the protein sample was thoroughly mixed with 4×LDS Sample Buffer and then denatured at 95°C for 5 min. Followed by: SDS-PAGE electrophoresis to separate protein samples, transfer protein from gel to PVDF membrane, 5% non-fat milk powder for non-specific background blocking, primary antibody incubation, secondary antibody incubation, ECL substrate catalytic luminescence, and X-ray film detection of protein bands. GAPDH which was used as the reference protein.

QUANTIFICATION AND STATISTICAL ANALYSIS

The screening criteria for core targets in PPI network was set as Degree UnDir > 11.04.

The results of GO enrichment analysis and KEGG signal pathway analysis were arranged in ascending order of p value, and the top 10 objects were selected successively. All p values were less than 0.01.

The screening criteria for key targets in Network of "matrine-core target-pathway" was set as Degree UnDir > 5.619.

All data were expressed as mean ± standard errors of the mean (mean ± SEM), where n represented the number of groups in the experiment and n=5. The analysis was performed using "One-way ANOVA" in GraphPad Prism version 8 software, and "Compared the mean of each column with the mean of every other columns" were selected for the analysis of differences between groups. "a, b, c, d, e" represented a significant difference between different columns ($p < 0.05$).